Hermans, J., & Acampora, A. (1967) *J. Am. Chem. Soc. 89*, 1547–1552.
Horbett, T. A., & Teller, D. C. (1973) *Biochemistry 12*, 1349–1358.
Johnson, M. L., & Frasier, S. G. (1985) *Methods Enzymol. 117*, 301–342.
Linderstrom-Lang, K., & Nielsen, S. O. (1959) in *Electrophoresis* (Bier, M., Ed.) Vol. 1, pp 35–89, Academic, New York.
Martin, C. J. (1964) *Biochemistry 3*, 1635–1643.
Martin, C. J. & Frazier, A. R. (1963) *J. Biol. Chem. 238*, 3268–3273.
Neet, K. E., & Brydon, S. E. (1970) *Arch. Biochem. Biophys. 136*, 223–227.
Nozaki, Y., & Tanford, C. (1967a) *Methods Enzymol. 11*, 715–734.
Nozaki, Y., & Tanford, C. (1967b) *J. Am. Chem. Soc. 89*, 736–742.
Nozaki, Y., & Tanford, C. (1967c) *J. Am. Chem. Soc. 89*, 742–749.
Pace, C. N. (1975) *CRC Crit. Rev. Biochem. 3*, 1–43.
Pace, C. N. (1986) *Methods Enzymol. 131*, 266–280.
Pace, C. N., & Vanderburg, K. E. (1979) *Biochemistry 18*, 288–292.
Pfeil, W., & Privalov, P. L. (1976) *Biophys. Chem. 4*, 23–32.
Rossotti, F. J. C., & Rossotti, H. (1965) *J. Chem. Educ. 42*, 375–378.
Roxby, R. W. (1970) *Conformational Effects on the Proton Equilibria of Lysozyme*, University Microfilms, Ann Arbor, MI.
Roxby, R., & Tanford, C. (1971) *Biochemistry 10*, 3348–3352.
Santoro, M. M. & Bolen, D. W. (1988) *Biochemistry* (preceding paper in this issue).
Schellman, J. A. (1978) *Biopolymers 17*, 1305–1322.
Schellman, J. A. (1987) *Annu. Rev. Biophys. Biophys. Chem. 16*, 115–137.
Schellman, J. A., & Hawkes, R. B. (1980) in *Protein Folding* (Jaenicke, R., Ed.) pp 331–343, Elsevier, New York.
Steinhardt, J., & Zaiser, E. M. (1955) *Adv. Protein Chem. 10*, 151–226.
Tanford, C. (1950) *J. Am. Chem. Soc. 72*, 441–451.
Tanford, C. (1955) in *Electrochemistry in Biology and Medicine* (Shedlovsky, T., Ed.) pp 248–265, Wiley, New York.
Tishchenko, V. M., Tiktopulo, Y. I., & Privalov, P. L. (1974) *Biofizika 19*, 400–404.

Crystal Structure of Nitric Oxide Inhibited Cytochrome *c* Peroxidase†

Steven L. Edwards*,‡ and Joseph Kraut
Department of Chemistry, University of California—San Diego, La Jolla, California 92093
Thomas L. Poulos
Center for Advanced Research in Biotechnology, 9600 Gudelsky Drive, Rockville, Maryland 20850
Received May 2, 1988; Revised Manuscript Received July 1, 1988

ABSTRACT: We have collected X-ray diffraction data from a crystal of cytochrome *c* peroxidase (CCP) complexed with the inhibitor nitric oxide to a resolution of 2.55 Å. A difference Fourier map shows density indicating the NO ligand is bound to the heme iron at the sixth coordination site in a bent configuration. Structural adjustments were determined by least-squares refinement that yielded an agreement residual of $R = 0.18$. The orientation of the ligand, tilting toward Arg-48, causes adjustment in the position of this nearby polar side chain. As a model for the substrate hydrogen peroxide, this geometry is consistent with the suggestion that Arg-48 serves to polarize the O–O peroxide bond to promote heterolytic cleavage of the bond [Poulos, T. L., & Kraut, J. (1980) *J. Biol. Chem. 255*, 8199–8205]. Strong difference density is also observed near residues 190–194, especially around the indole ring of Trp-191. The density indicates movement of the indole ring away from the proximal His-175 imidazole ring by about 0.25 Å, which appears to cause perturbation of the neighboring residues. The response of Trp-191 on the proximal side of the heme to binding nitric oxide on the distal side probably results from delocalization of the electron density of the ligand. Relevant to this is the recent finding that a mutant in which Trp-191 is replaced by phenylalanine has dramatically reduced activity, less than 0.05% of the parent activity [Mauro, J. M., Fishel, L. A., Hazzard, J. T., Meyer, T. E., Tollin, G., Cusanovich, M. A., & Kraut, J. (1988) *Biochemistry 27*, 6243–6256]. Characterization of this mutant showed in particular that electron transfer from cytochrome *c* was severely hindered. This mutagenesis result combined with the sensitivity of the position of Trp-191 to the electronic character of the sixth coordination site ligand leads us to speculate on the role of Trp-191 in electron transfer.

Cytochrome *c* peroxidase (ferrocytochrome *c*:H_2O_2 oxidoreductase, EC 1.11.1.5; CCP)[1] is easily isolated from the mitochondria of yeast (Yonetani & Ray, 1965). Early experiments demonstrated its ability to rapidly catalyze the cleavage of organic hydroperoxide molecules into alcohol and

† This work was supported by National Science Foundation Grant DMB-8511656 awarded to J.K.
* Author to whom correspondence should be addressed.
‡ Present address: Center for Advanced Research in Biotechnology, 9600 Gudelsky Drive, Rockville, MD 20850.

[1] Abbreviations: CCP, cytochrome *c* peroxidase; ENDOR, electron nuclear double resonance; EPR, electron paramagnetic resonance; EXAFS, extended X-ray absorption fine structure.

0006-2960/88/0427-8074$01.50/0

water using cytochrome *c* as a source of electrons (Abrams et al., 1942). Further work showed that CCP had many properties in common with the two well-studied classes of heme proteins: the cytochromes and the globins. Similarity of structure between CCP and the globins was suggested by the fact that certain heme-binding inhibitors of myoglobin and hemoglobin, including nitric oxide, also inhibit CCP to yield complexes with absorption spectra similar to those of inhibited globin complexes (Yonetani & Ray, 1965). Moreover, CCP has been shown to be able to substitute for the terminal oxidase in yeast when the latter is inactivated by carbon monoxide (Erecinska et al., 1973). These properties of CCP, including its ease of crystallization, recommend it as a model for the study of cytochrome oxidase, which is more complicated and difficult to crystallize.

The reaction catalyzed by CCP, including intermediate states, is

$$\text{CCP} + \text{ROOH} \rightarrow \text{compound I} + \text{ROH}$$

$$\text{compound I} + \text{cyt-}c(\text{Fe}^{2+}) + \text{H}^+ \rightarrow \text{compound II} + \text{cyt-}c(\text{Fe}^{3+})$$

$$\text{compound II} + \text{cyt-}c(\text{Fe}^{2+}) + \text{H}^+ \rightarrow \text{CCP} + \text{cyt-}c(\text{Fe}^{3+}) + \text{H}_2\text{O}$$

where ROOH is an alkyl peroxide or hydrogen peroxide. As implied by the above scheme, CCP provides two reducing equivalents required to cleave the peroxide bond, itself being oxidized to a semistable intermediate termed compound I (Jordi & Erman, 1974). Two one-electron transfers from cytochrome *c* reduce compound I back to the parent state. We will use the term "parent" to refer to resting ferric CCP. Compound I of CCP is an unusual intermediate because its long half-life, about 4 h at room temperature (Erman & Yonetani, 1975), has allowed it to be examined by a variety of experimental techniques. These experiments suggest that one of the reducing equivalents lost upon formation of compound I is contributed by the heme iron, which is oxidized from the ferric to the ferryl state (Lang et al., 1976). The donor of the second equivalent is believed to be some configuration of amino acid side chains (Yonetani et al., 1966; Hoffman, et al., 1979; Edwards et al., 1987), which when oxidized manifests itself by an intense free radical type EPR signal (Yonetani et al., 1966).

As already noted, spectroscopic measurements on CCP complexed with certain inhibitors suggest a heme environment similar to that of the globins (Yonetani & Ray, 1965). Nitric oxide (NO) binds to CCP with its heme iron in either the ferrous or the ferric state. EPR analysis of NO bound to *ferrous* CCP yielded spectra that allowed identification of the fifth coordination ligand as the imidazole nitrogen of a histidine residue (Yonetani et al., 1972). An important conclusion of this work was that the unpaired electron of the NO ligand is substantially delocalized over the iron and the imidazole ring of the proximal histidine. In addition, NO bound to *ferric* CCP is diamagnetic, indicating that the unpaired electron of NO is essentially transferred to the iron, yielding an electronic configuration that may be described as Fe^{2+}–NO^+ (Ehrenberg & Szczepkowski, 1960; Yonetani et al., 1972).

We have previously reported crystal structures of three inhibitor complexes: the complexes of CCP with cyanide (Poulos et al., 1978), nitric oxide (Edwards, 1981), and fluoride (Edwards et al., 1984). The two earlier papers suffered to some extent because they were interpreted by using the atomic coordinates of the original parent structure which, in fact, included some errors that were subsequently corrected. The parent structure has since been refined against 1.7-Å data, yielding an *R* factor of 0.20 and standard geometry (Finzel et al., 1984). With the refined structure now in hand, it is appropriate to reexamine the inhibitor complexes. One of these, ferric CCP inhibited by nitric oxide, is especially provocative because it appears to show structural perturbations on the proximal side of the heme in the same vicinity as noted for compound I (Edwards et al., 1987).

The identity of the free radical site in CCP compound I has remained elusive for years despite the analysis of many careful experiments. Two strong candidates for the radical site have been Trp-51 (Poulos & Kraut, 1980a) and Met-172 (Hoffman et al., 1980). A powerful new tool engaged to test these choices is site-directed mutagenesis. Results of mutagenesis experiments now demonstrate that the radical site is neither Trp-51 (Fishel et al., 1987) nor Met-172 (Goodin et al., 1986). The experiment described here in conjuction with the crystallographic examination of compound I (Edwards et al., 1987) leads us to believe that the radical site may involve residues near the proximal histidine, in particular Trp-191 and methionines 230–231. Additional support for this assignment comes from a mutagenesis experiment in which Trp-191 was replaced by a phenylalanine (Mauro et al., 1988).

Experimental Procedures

Cytochrome *c* peroxidase was purified from bakers' yeast by the method of Nelson et al. (1977). Parent CCP crystals were grown by established methods (Poulos et al., 1978). A nitric oxide solution was prepared by flowing NO gas over a small beaker of synthetic mother liquor and readjusting the pH to 6.0 by the addition of potassium hydroxide. The synthetic mother liquor was 50 mM potassium phosphate buffered at pH 6.0 and 30% v/v 2-methyl-2,4-pentanediol. The complex formed spontaneously when a parent CCP crystal was added to this solution. A crystal prepared in this manner was mounted in a glass capillary that was then fixed on an Enraf-Nonius CAD-4 diffractometer equipped with an Enraf-Nonius fine-focus sealed copper tube that was operated at 40 mA and 36 kV using a Ni filter. An orientation matrix was determined by an automated reflection searching routine that calculated the cell dimensions as $a = 107.52$, $b = 76.56$, and $c = 51.69$ Å, $\alpha = \beta = \gamma = 90.0°$ in space group $P2_12_12_1$. These dimensions are essentially the same as those of the parent cell with the largest difference being the *c* axis, where the parent has $c = 51.43$ Å. Data were collected at room temperature (20 °C).

From one crystal, 13 785 unique reflections were measured in θ–2θ geometry to form a data set that is complete to 2.55 Å. Decay of the crystal was monitored by periodic measurement of four reference reflections chosen to represent different regions of reciprocal space. At the end of data collection the average decay for the reference reflections was 30%. We note that scattering ability and resistance to X-ray-induced decay appeared to be significantly better for the NO complex than for parent CCP crystals examined under similar conditions. Following data collection, an empirical absorption correction was determined by choosing a strong reflection whose scattering vector was nearly collinear with the ϕ axis and measuring the variation of its intensity while the crystal was rotated around its scattering vector a full 360°. The background level as a function of 2θ was estimated by collecting counts for 2.5 min at increasing detector angles while the crystal was adjusted away from any diffracting conditions. The data were collected in 11 shells defined by 2θ limits chosen so that adjacent shells would overlap by approximately 50 reflections to allow for proper scaling. After the reflection measurements were corrected for absorption, background and

FIGURE 1: CCP nitric oxide complex minus parent cytochrome *c* peroxidase difference Fourier map superimposed on a backbone model of the parent structure. Contour levels are at $\pm 4\sigma$ with positive contours shown with solid lines and negative contours with broken lines.

Lorentz and polarization effects, the data were scaled together by using 953 observations of 368 unique reflections which yielded a residual of 3.5% based on intensities. Subsequent calculations were carried out by using the XTAL system of computer programs (Hall et al., 1980).

The starting model for refinement of the CCP–NO complex was the refined parent structure (Finzel et al., 1984). We applied the conjugate-gradient least-squares procedure of Hendrickson and Konnert (1980) as described by Finzel et al. (1984) with the following exceptions: the target σ value for bond lengths was reduced to 0.020 Å, and the target value for distances related to bond angles (1–3 type) was reduced to 0.030 Å to ensure proper geometry. In addition, we note that we used a form of the Hendrickson and Konnert program, PROLSQ, that includes a fast Fourier transform (FFT) implemented by Finzel (1987). This FFT version of the program does not allow the use of an amorphous water correction, and therefore the lowest resolution data were not used ($d > 20$ Å). However, our experience using this version of the program compared to the non-FFT version in test refinements has shown that it produces identical results within the expected parameter error while yielding at least a 5-fold increase in speed on a VAX 11/750 computer.

The difference between the *c* cell dimension of parent CCP and the NO complex is small, 0.26 Å, but not small enough to ignore completely. Therefore, two sets of refinement calculations were carried out, one using the parent unit cell dimensions and the other using the unit cell dimensions of the complex. The resulting structures from both calculations were nearly identical. The magnitudes of some positional adjustments relative to the parent were slightly different; in these instances we report the more conservative values. The refinement using unit cell dimensions of the complex and all of the data from 20 to 2.55 Å converged with a residual of 0.18. The average parameter shift of the complex with respect to the parent was 0.64 Å. The resulting geometry included 314 distances larger than 2 times the σ target values and one distance larger than 5σ. By conventional standards (Luzzati, 1952) the average coordinate error may be as high as 0.25 Å. However, since the coordinates shifted during refinement by a very small amount from the parent, which is well determined at higher resolution, 1.7 Å, the actual error is probably smaller.

We were particularly interested in trying to determine the positions of the iron, the NO ligand, and the residues around Trp-191. Consequently, additional cycles of refinement were run with these atoms removed from the model in order to calculate unbiased phases. Various $F_o - F_c$ maps based on this type of refinement were used to estimate positions for the deleted parts of the molecule. In addition, after positions for the NO ligand atoms were determined from difference maps, these atoms were reinserted into the model for further cycles of refinement to confirm the estimate of the Fe–N–O bond angle. In this case the ligand-related bond distances, Fe–N and N–O, were constrained to 1.75 and 1.10 Å, respectively, as suggested by a small-molecule heme X-ray structure that also included NO as a ligand (Piciulo et al., 1974).

The $F_o - F_o$ map used all of the data from infinity to 2.55 Å, while the $F_o - F_c$ maps had the data below 20 Å omitted because of the restricted resolution range used for refinement. All data set scaling was done with single scale factors plus a temperature scale factor.

RESULTS

The difference Fourier map, CCP–NO complex minus parent, using computed phases of the parent, is shown in Figure 1. The map is contoured at $\pm 4\sigma$, where σ is defined to be the rms difference density for the entire unit cell. It can be seen that most of the difference density is located near the ligand binding pocket and on the proximal side of the heme, somewhat below the propionates. A close-up view of the heme vicinity is shown in Figure 2. The largest feature of the map is a peak near the heme axis due to the nitric oxide ligand. Binding of the ligand also causes positional adjustments of the heme iron and of the side chains that make up the binding pocket. In addition, positional adjustments on the proximal side of the heme around Trp-191 are suggested by the difference map shown in two different views in Figures 2 and 3. For identification of additional residues see Figure 4. We will describe the adjustments around the ligand binding pocket first and those near Trp-191 afterward.

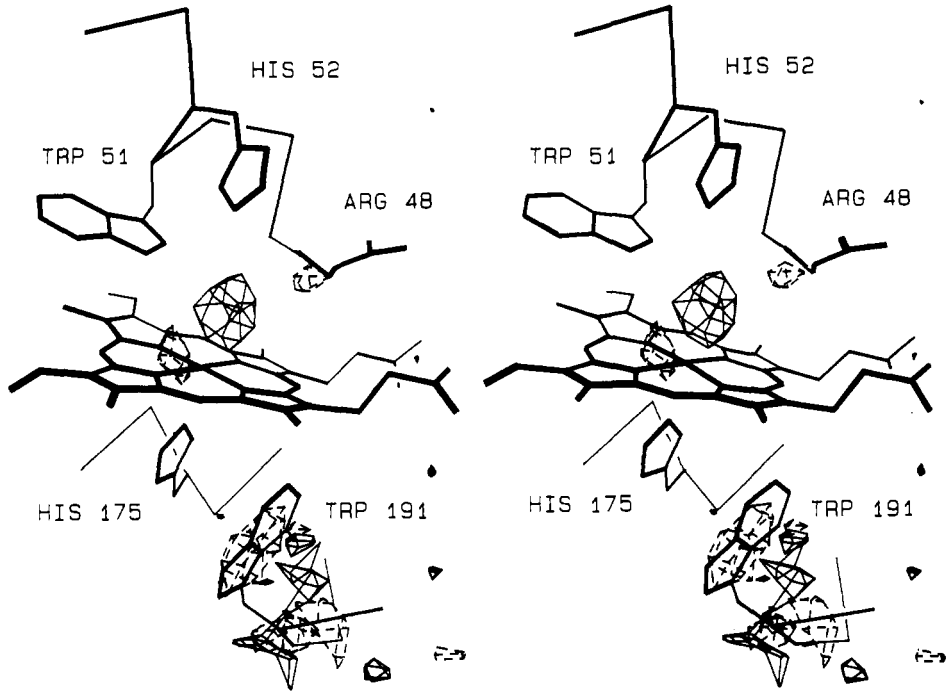

FIGURE 2: Magnified view of the CCP nitric oxide complex minus parent CCP difference Fourier map emphasizing the density around the ligand binding site and around Trp-191 seen here below the heme. Contours are at $\pm 4\sigma$ with the positive density shown with solid lines and the negative density with broken lines.

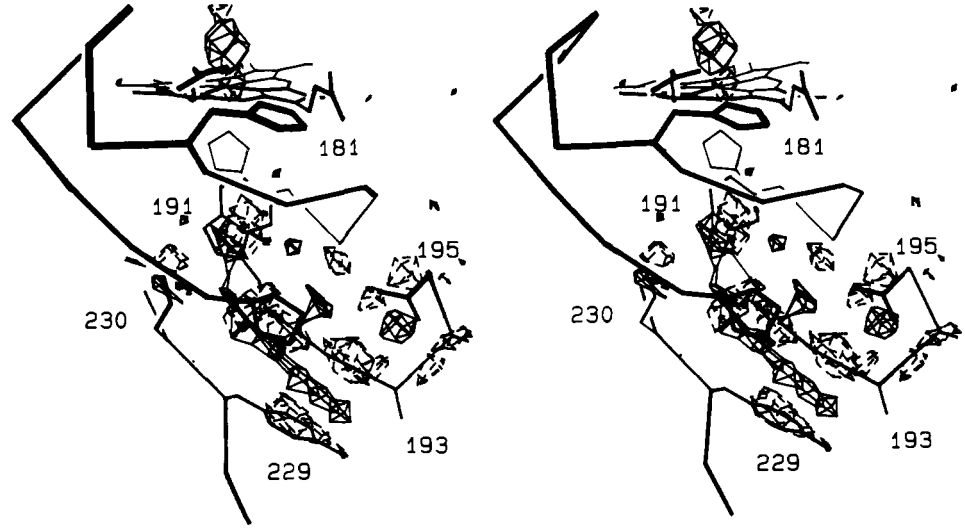

FIGURE 3: Another view of the difference Fourier map on the proximal side of the heme approximately 90° away from the view of Figure 2 and at the same contour level. This view emphasizes the difference density around residues 190–195. The extended loop shown to support His-181 forms part of the binding surface for cytochrome *c* in the hypothetical model for the electron-transfer complex (Poulos & Kraut, 1980b). Other numbered residues shown are Trp-191, Ala-193, Gln-195, Tyr-229, and Met-230.

In Figure 2, the density near the heme axis represents the oxygen of the nitric oxide ligand. EPR analysis of the NO complex with CCP indicates that the nitrogen atom of the ligand coordinates to the heme iron (Yonetani et al., 1972). This approximate position is occupied by a fixed water molecule in the parent structure, Wat-595. Because of the position and electron density of this water molecule, the nitrogen atom of the ligand fails to show up in the difference map. The peak of the ligand density is slightly off the heme axis, indicating that the ligand is bound in a bent configuration. An attempt to measure the Fe–N–O angle was made by removing the two water molecules near the nitric oxide binding site, Wat-595 and Wat-648, from the parent structure and refining the remaining structure against the observed data. The purpose of this maneuver was to produce phases that were not biased by the two water molecules. When the refinement had converged, an $F_o - F_c$ difference Fourier map using calculated phases revealed an ellipsoid-shaped feature of density near the heme axis representing both atoms of the NO ligand. The geometry of the ligand was modeled by placing a nitrogen atom on the heme axis 1.75 Å from the iron. A second atom representing the oxygen atom was rotated around the first atom tethered

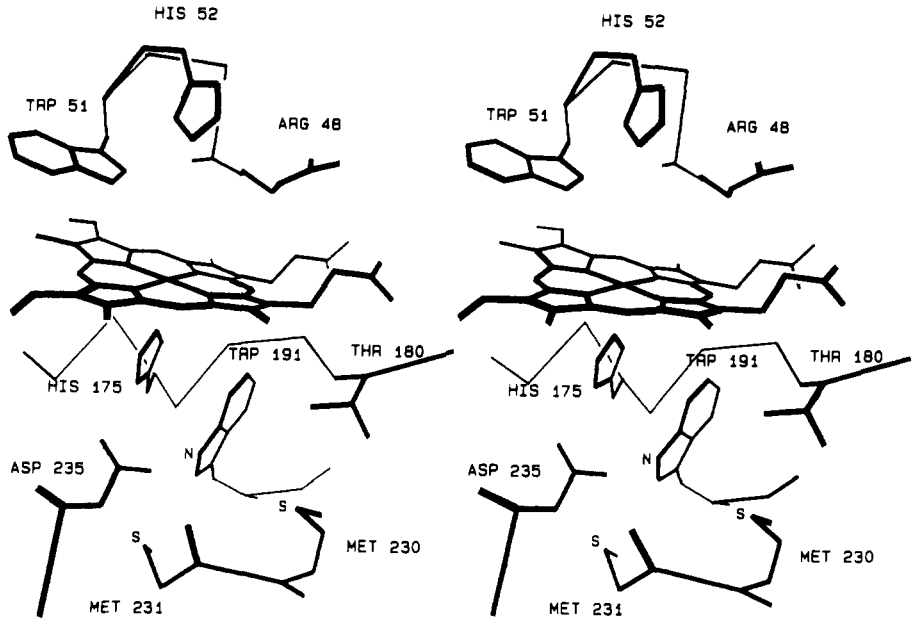

FIGURE 4: Identification of additional residues around the heme in CCP emphasizing the position of Trp-191 relative to the sulfur atoms of the methionine pair, 230–231. Trp-191 and the methionine pair have been suggested as the site of the free radical in compound I.

at a distance of 1.10 Å until it overlapped the difference density at the highest value. The resulting Fe–N–O bond angle was estimated to be 130 (10)°. Finally, automated refinement of the ligand geometry was attempted. The nitric oxide atoms were incorporated into the model starting at positions estimated by manual fitting and constrained by the bond distances used in the manual fitting. After four cycles of refinement, the positions of the ligand atoms had changed by an average of 0.15 Å. The resulting Fe–N–O angle measured 143 (12)°. When the N–O bond is projected onto the heme plane, it comes within 5° of eclipsing the bond from the iron to the nitrogen of pyrrole ring 4.

The presence of the NO ligand tends to push away the side chains that form the binding pocket. The oxygen atom of the ligand tilts toward the side chain of Arg-48. Negative density near the Nε of Arg-48 shows that its side chain moves away from the ligand in the complex. The result is confirmed by the structure refinement which shows that Nε of Arg-48 moves about 0.5 Å away from the ligand, separating it by about 3.4 Å from the NO oxygen atom. This distance is probably too large for a hydrogen bond. However, in the $F_o - F_c$ map, a moderate-sized peak at the position of Wat-648 reappeared even though this water had been removed from the structure. The center of this peak is 2.8 Å from Nζ1 or Arg-48 and 2.8 Å from the oxygen position of the NO ligand. This peak presumably represents a water molecule with an occupancy of 25–50%, as judged from its size. Its location may indicate a partially occupied Wat-648 forming a hydrogen bond to either the ligand or Arg-48 or both. The nature of this water may require higher resolution data to be properly understood.

The other side chains that make up the ligand binding pocket, Trp-51 and His-52, also move away from the NO ligand. The indole ring of Trp-51 moves away by an average distance of 0.25 Å, which also causes it to move slightly further from the heme ring. The imidazole ring of His-52 moves upward in a direction parallel to the heme axis by an average of 0.30 Å.

The position of the heme iron was determined by removing it from the model and performing three cycles of refinement in order to calculate phases unbiased by its position in the parent structure or by any restraints included in the refinement program. Subsequently, an $F_o - F_c$ map calculated with these new phases showed a peak for the iron position. The highest point of this peak (24 σ) is situated exactly in the plane of the heme pyrrole nitrogens. Afterward, the refinement was rerun including the iron in the model, and the iron indeed moved from its initial position in the parent structure to the position of the difference-map peak just described. Thus, in the parent enzyme, the iron atom resides 0.2 Å to the proximal side of the heme (Finzel et al., 1984) but when bound to the nitric oxide ligand, it moves directly into the plane of the heme.[2] According to the refinement, the proximal His-175 imidazole ring does not move. Therefore, the imidazole Nε–Fe distance increases from 2.0 Å in the parent to 2.2 Å in the complex.

The second largest feature in the difference map is an envelope of negative density around the indole ring of Trp-191 (see Figure 2). Adjacent to this envelope is a cluster of positive density peaks on the side of the indole ring away from the proximal histidine. This pattern of positive and negative density indicates that the indole ring moves away from the proximal histidine imidazole ring in the NO complex relative to its position in the parent structure. The magnitude of this motion was calculated by the refinement to be 0.25 Å. In addition, there is strong positive and negative difference density stretching along the backbone of residues 190–194 (see Figure 3). The general direction implied for this movement is away from the proximal histidine, His-175, and the impetus for it appears to be the adjustment of the Trp-191 indole ring. The magnitude of the adjustment of these residues after six cycles of refinement was surprisingly small. In addition an $F_o - F_c$ map calculated following the six refinement cycles showed that many peaks and holes persisted in this area. We suspected that the refinement may have been trapped in a false minimum. To resolve this question, residues 190–193 were removed from the model and three more cycles of refinement were performed. A new $F_o - F_c$ map was calculated, but the density for these residues merely confirmed the result of the refine-

[2] We note that in our earlier paper describing the structure of CCP compound I (Edwards et al., 1987) we stated *incorrectly*, in a reference to the CCP–NO complex, that the iron maintains the same position as in the parent, 0.2 Å to the proximal side of the heme. Following analysis by least-squares refinement, we now believe that in fact the iron moves into the heme plane in the NO complex.

ment. We interpret this to mean that these residues become less ordered in the complex but that their new average positions are not much different from their positions in the parent. This interpretation is underscored by the increase in temperature factors for the backbone atoms of this segment. The parent and NO complex structures have nearly identical overall temperature factors, 24 Å^2, but along the segment 189–195 the backbone-atom temperature factors in the complex increase dramatically; all have values over 30 Å^2, and they reach a maximum of over 40 Å^2 at residue 193. It is interesting that most of these residues except for Trp-191 have short side chains; the sequence for 189–195 is Gly-Pro-Trp-Gly-Ala-Ala-Gln.

Difference density also appears close to the phenol ring of Tyr-229 and the side chain of Met-230, which are adjacent to residues 191–193. The refinement indicates that the Met-230 side chain moves 0.25 Å away from the indole ring of Trp-191 while the phenol ring of Tyr-229 moves 0.30 Å toward the backbone atoms of Gly-192. In contrast to residues 189–195, the backbone atoms of these two residues do not change significantly in position or temperature factor.

Discussion

Nitric oxide is a useful probe for investigating the ligand environment in heme proteins (Kon & Kataoka, 1969). Since NO has an unpaired electron, the complex of heme proteins with NO can be analyzed by EPR spectroscopy when the iron is in the *ferrous* state. In contrast, when NO binds to *ferric* heme iron, which is the enzymically relevant state for CCP, the unpaired electron is effectively transferred to the iron, where it couples with the unpaired electron of the d^5 iron making the complex EPR silent (Yonetani et al., 1972). Is the unpaired electron from the NO ligand localized on the heme iron, or is some of its electron density delocalized to an area that includes the proximal histidine? The crystal structure of the ferric CCP–NO complex shows perturbations adjacent to the proximal histidine, suggesting that some of the electron density may be delocalized. The difference Fourier map and refinement of the structure indicate that the indole ring of Trp-191 moves by 0.25 Å away from the imidazole ring of its neighbor, His-175.

Why should the Trp-191 indole ring move away from the proximal histidine ring when NO binds the sixth coordination site? The indole ring and the imidazole ring both donate hydrogen bonds to the same buried charge group, Asp-235 (Poulos et al., 1980). It may be argued that this promotes some negative charge character on one or both rings. In fact, a resonance Raman spectroscopic examination of CCP suggests a significant population of His-175 in the form of an imidazolate anion (Giulietta Smulevich, personal communication). If so, increased electron charge from the NO ligand may cause the two negatively charged rings to repel each other. Regardless of the details, it seems clear that Trp-191 is responding to a change in its environment brought about by the presence of the nitric oxide ligand. Since there is no evidence to suggest that this response is the result of any direct structural perturbation due to the ligand, the connection between Trp-191 and the NO ligand appears to be electronic in nature.

The crystal structure of CCP compound I, in striking parallel to the results obtained here for the CCP–NO complex, also revealed perturbations of residues in the same vicinity on the proximal side of the heme (Edwards et al., 1987). In that experiment, a difference Fourier map calculated between the compound I and parent diffraction data showed strong difference density near the side chain of Thr-180, a neighbor of Trp-191 (see Figure 4). Also present in this vicinity as close neighbors of Trp-191 are the methionines Met-230 and Met-231. It may be recalled that, on the basis of ENDOR measurements, a pair of closely juxtaposed methionine sulfur atoms sharing a positive charge was originally proposed for the radical site by Hoffman and co-workers (Hoffman et al., 1979). This idea was later discarded in view of the large distance between the methionine sulfurs and the heme iron, over 10 Å (Poulos et al., 1980) and the separation of 6.5 Å between the two methionine sulfurs. Because the CCP compound I and NO complex crystal results demonstrated that oxidation and reduction of the heme iron cause adjustments in this vicinity, it appeared that Hoffman's proposal of a pair of methionines supporting a cationic radical merited reconsideration. Crystallographic refinement of the compound I structure indicated that the side-chain oxygen of Thr-180 and two backbone carbonyl oxygen atoms had moved toward the Met-230 sulfur, perhaps responding to a partial positive charge on the sulfur. The strategic location of Trp-191, with its indole nitrogen between the sulfurs of the methionine pair, Met-230 and Met-231, and hydrogen bonded to the buried charge group, Asp-235, suggested that it participates in the formation or the stabilization of the compound I radical. This idea has been examined by a mutagenesis experiment in which Trp-191 was replaced by a phenylalanine (Mauro et al., 1988). The mutant displayed a radical-type EPR signal readily on reaction with peroxide, but this radical site was judged to be 100-fold less stable than that manifested by the parent. The activity of the Phe-191 mutant was dramatically reduced to 0.05% of the parent enzyme's activity, but the reduced activity was ascribed to impeded electron transfer with cytochrome *c*. For comparison, the Phe-51 mutant that also had a less stable compound I showed no decrease in catalytic activity (Fishel et al., 1987). Mauro and co-workers propose that Trp-191 may be part of a specific pathway that links the heme centers of CCP and cytochrome *c*. However their results so far do not confirm or deny whether Trp-191 is by itself or by interaction with neighbors the radical site (Mauro et al., 1988).

In our paper on the compound I crystal experiment (Edwards et al., 1987) we described how oxidation of the proposed radical site and the heme iron caused a loop made up of residues 175–191 to twist. The relevance of this loop twist is that it appears to link structural adjustments at its two ends, 175 and 191, near the heme iron to an adjustment at the surface of the molecule where cytochrome *c* has been proposed to bind in an electron-transfer complex (Poulos & Kraut, 1980b). Reciprocally, it may also be possible that formation of the electron-transfer complex may induce a structural adjustment of the heme iron environment via the 175–191 loop that is more conducive to electron transfer. This follows the theory of Marcus that electron transfer between proteins may require small structural adjustments (Marcus, 1982). We have described how the Trp-191 indole ring is perturbed in the CCP–NO complex and that residues 192–194 appear to be flexible as evidenced by increased temperature factors. For the sake of erecting a working hypothesis, it could be proposed that residues 175–191 relay the structural adjustment caused by the formation of the electron-transfer complex toward the heme environment, especially to Trp-191, while residues 192–194 by virtue of their flexibility allow the Trp-191 indole ring to rotate into a better position to facilitate electron transfer.

The nitric oxide ligand binds to the heme iron with bent geometry. On the basis of refinement, the Fe–N–O angle was determined to be 143 (12)°. This is the same as the Fe–N–O angle found in the small-molecule structure of nitrosyl(tet-

raphenylporphinato)(1-methylimidazole)iron (Piciulo et al., 1974) and within the estimated error of the angle for nitric oxide bound to hemoglobin (Deatherage & Moffat, 1979). We caution that in the latter two structures the oxidation state of the iron was Fe^{2+}, whereas in our case it is formally Fe^{3+}. Nitric oxide has been shown to bind to various metals in both bent and linear geometries, and it is difficult to predict which will be preferred in each case. A rule for predicting the geometry based on the number of d electrons of the metal has been proposed based on molecular orbital calculations (Mingos, 1973). Applying this rule to NO bound to ferric iron predicts linear geometry, while NO bound to ferrous iron should be bent. However, these calculations do not take into account the ligand environment provided by the CCP protein. A linear bond for the ligand in CCP would put the NO oxygen in contact with the distal His-52. It is likely that the difference in energy between the bent and linear geometries for the NO ligand is small enough that other considerations like steric contacts and possible hydrogen bonds exert a significant influence on the ligand orientation.

When coordinated to nitric oxide, the heme iron moves 0.2 Å into the plane of the heme. This was unexpected from mere inspection of the difference Fourier (see Figure 2), which shows only slight density around the iron. However, refinement of the structure and a partial difference Fourier map corroborate movement of the iron from the proximal side into the plane of the pyrrole nitrogens. This is similar to the structure observed for NO bound to ferroheme in small-molecule crystallographic studies which show that the iron actually resides 0.07 Å out of the plane of the pyrrole nitrogens toward the NO ligand (Piciulo et al., 1974).

Why should the iron move in the presence of NO? Nitric oxide induces the heme iron to become low spin. According to one theory (Hoard, 1975), low-spin iron has a smaller electron orbital radius than high-spin iron and should therefore fit more easily into the porphyrin ring hole. More recent theories emphasize the strengths of the bonds that the iron atom makes with the axial ligands govern the position of the iron atom relative to the heme plane (Perutz, 1979). In the case of the CCP–NO complex, the bond to the NO nitrogen is probably short, 1.75 Å (Piciulo et al., 1974), compared to the iron to water bond distance in the parent structure, 2.4 Å (Finzel et al., 1984), and accordingly the iron atom is pulled into the plane of the heme when bound to NO. In addition, the iron to proximal imidazole nitrogen bond distance is longer, 2.2 Å compared to 2.0 Å in the parent, suggesting that the increased electron density from the NO ligand may have weakened the bond to the proximal histidine. For comparison, we cite the geometry of the iron in CCP compound I, where the ferryl iron is bound to an oxygen atom at the sixth coordination site. In this case, the ferryl oxygen bond distance is very short, 1.67 Å (Chance et al., 1986), which causes the iron to move 0.1 Å toward the distal side of the heme (Edwards et al., 1987).

Finally, we ask what the geometry of the NO ligand in the complex might tell us about the binding of peroxide to CCP. Nitric oxide is a diatomic molecule that binds to ferric iron in CCP with bent geometry as hydrogen peroxide most likely does. The NO ligand will become partially positively charged if it contributes its unpaired electron to the iron as suggested by EPR measurements (Yonetani et al., 1972). Due to this partial positive charge, it might be expected that the ligand would rotate to maximize its distance from the positive charge of Arg-48. However, the oxygen of the ligand points in the direction of Arg-48, while the arginine side chain moves by over 0.5 Å further away from the ligand binding site. It would appear possible that the NO ligand oxygen atom could have displaced Wat-596 and thus could have pointed away from Arg-48. However, the ligand binding pocket must be constructed in a way that causes a diatomic ligand to prefer the opposite orientation, pointed toward Arg-48. We emphasize this because it is the orientation proposed for the binding of hydrogen peroxide that would allow the positive charge of the Arg-48 guanidinium group to promote heterolytic cleavage of the peroxide bond (Poulos & Kraut, 1980a).

ACKNOWLEDGMENTS

We thank J. Matthew Mauro and his co-workers for making available valuable information about the CCP Phe-191 mutant prior to its publication. We also thank Stephen Dempsey for his ongoing development of the Molecular Modeling System graphics program used here to analyze results and prepare figures.

Registry No. L-Trp, 73-22-3.

REFERENCES

Abrams, R., Altschul, A. M., & Hogness, T. R. (1942) *J. Biol. Chem. 142*, 303–316.

Chance, M., Powers, L., Poulos, T., & Chance, B. (1986) *Biochemistry 25*, 1266–1270.

Coulson, A. F., & Yonetani, T. (1972) *Biochem. Biophys. Res. Commun. 49*, 391–398.

Deatherage, J. F., & Moffat, K. (1979) *J. Mol. Biol. 134*, 401–417.

Dolphin, D., Forman, A., Borg, D. C., Fajer, J., & Felton, R. H. (1971) *Proc. Natl. Acad. Sci. U.S.A. 68*, 614–618.

Edwards, S. L. (1981) Ph.D. Dissertation, University of California—San Diego.

Edwards, S. L., Poulos, T. L., & Kraut, J. (1984) *J. Biol. Chem. 259*, 12984–12988.

Edwards, S. L., Xuong, Ng.H., Hamlin, R. C., & Kraut, J. (1987) *Biochemistry 26*, 1503–1511.

Ehrenberg, A., & Szczepkowski, T. W. (1960) *Acta Chem. Scand. 14*, 1684–1692.

Erecinska, M., Oshino, N., Loh, P., & Brocklehurst, E. (1973) *Biochim. Biophys. Acta 292*, 1–12.

Erman, J. E., & Yonetani, T. (1975) *Biochim. Biophys. Acta 393*, 350–357.

Finzel, B. C. (1987) *J. Appl. Crystallogr. 20*, 53–55.

Finzel, B. C., Poulos, T. L., & Kraut, J. (1984) *J. Biol. Chem. 259*, 13027–13036.

Fishel, L. A., Villafranca, J. E., Mauro, J. M., & Kraut, J. (1987) *Biochemistry 26*, 351–360.

Fujita, I., Hanson, L. K., Walker, F. A., & Fajer, J. (1983) *J. Am. Chem. Soc. 105*, 3296–3300.

Goodin, D. B., Mauk, A. G., & Smith, M. (1986) *Proc. Natl. Acad. Sci. U.S.A. 83*, 1295–1299.

Hall, S. R., Stewart, J. M., & Munn, R. J. (1980) *Acta Crystallogr., Sect. A: Cryst. Phys., Diffr., Theor. Gen. Crystallogr. A36*, 979–989.

Hendrickson, W. A., & Konnert, J. H. (1980) in *Computing in Crystallography* (Diamond, R., Ramaseshan, S., & Venkatesan, K., Eds.) pp 13.1–13.23, Indian Institute of Science, Bangalore, India.

Hoard, J. L. (1971) *Science (Washington, D.C.) 174*, 1295–1302.

Hoffman, B. M., Roberts, J. E., Brown, T. G., Kang, C. H., & Margoliash, E. (1979) *Proc. Natl. Acad. Sci. U.S.A. 76*, 6132–6136.

Hoffman, B. M., Roberts, J. E., Kang, C. H., & Margoliash, E. (1981) *J. Biol. Chem. 256*, 6556–6564.

Jordi, H. C., & Erman, J. E. (1974) *Biochemistry 13*, 3734–3741.
Kon, H., & Kataoka, N. (1969) *Biochemistry 8*, 4757–4562.
Lang, G., Spartalian, K., & Yonetani, T. (1976) *Biochim. Biophys. Acta 451*, 250–258.
Luzzati, V. (1952) *Acta Crystallogr. 5*, 802–810.
Marcus, R. A. (1982) *Oxidases and Related Redox Systems* (King, T. E., Mason, H. S., & Morrison, M., Eds.) pp 3–19, Pergamon, New York.
Mauro, J. M., Fishel, L. A., Hazzard, J. T., Meyer, T. E., Tollin, G., Cusanovich, M. A., & Kraut, J. (1988) *Biochemistry 27*, 6243–6256.
Mingos, D. M. P. (1973) *Inorg. Chem. 12*, 1209–1211.
Nelson, C. E., Sitzman, E. V., Kang, C. H., & Margoliash, E. (1977) *Anal. Biochem. 83*, 622–631.
Perutz, M. F. (1970) *Nature (London) 228*, 726–739.
Perutz, M. F. (1979) *Annu. Rev. Biochem. 48*, 327–386.
Piciulo, P. L., Rupprecht, G., & Scheidt, W. R. (1974) *J. Am. Chem. Soc. 96*, 5393–5395.
Poulos, T. L., & Kraut, J. (1980a) *J. Biol. Chem. 255*, 8199–8205.
Poulos, T. L., & Kraut, J. (1980b) *J. Biol. Chem. 255*, 10322–10330.
Poulos, T. L., Freer, S. T., Alden, R. A., Xuong, Ng.h., Edwards, S. L., Hamlin, R. C., & Kraut, J. (1978) *J. Biol. Chem. 253*, 3730–3735.
Poulos, T. L., Freer, S. T., Alden, R. A., Edwards, S. L., Skogland, U., Takio, T., Eriksson, B., Xuong, Ng.h., Yonetani, T., & Kraut, J. (1980) *J. Biol. Chem. 255*, 575–580.
Yonetani, T., & Ray, G. S. (1965) *J. Biol. Chem. 240*, 4503–4508.
Yonetani, T., & Ray, G. S. (1966) *J. Biol. Chem. 241*, 700–706.
Yonetani, T., Schleyer, H., & Ehrenberg, A. (1966) *J. Biol. Chem. 241*, 3240–3243.
Yonetani, T., Yamamoto, H., Erman, J. E., Leigh, J. S., & Reed, G. H. (1972) *J. Biol. Chem. 247*, 2447–2455.

Differential Scanning Calorimetric Study of the Thermal Denaturation of Aspartate Transcarbamoylase of *Escherichia coli*†

Victoria Edge and Norma M. Allewell
Department of Molecular Biology and Biochemistry, Wesleyan University, Middletown, Connecticut 06457
Julian M. Sturtevant*
Deparments of Chemistry and of Molecular Biophysics and Biochemistry, Yale University, New Haven, Connecticut 06520
Received October 30, 1987; Revised Manuscript Received June 27, 1988

ABSTRACT: The thermal denaturation of *Escherichia coli* aspartate transcarbamoylase (c_6r_6) in the absence and presence of various ligands has been studied by means of high-sensitivity differential scanning calorimetry (DSC). As previously reported [Vickers, K. P., Donovan, J. W., & Schachman, H. K. (1978) *J. Biol. Chem. 253*, 8493–8498], the denaturational endotherm consists of two peaks, the lower of which is due to denaturation of the three regulatory, r_2, subunits while the upper involves the two catalytic, c_3, subunits. The temperature of maximal excess apparent specific heat, t_m, of the lower peak is raised from the value of 51.4 °C for the isolated subunit to 66.8 °C as a result of subunit interactions, whereas t_m for the c_3 peak is essentially the same in the isolated subunit and in the holoenzyme, indicating that the denatured r_2 subunits do not interact with the c_3 subunits. The total specific denaturational enthalpy for c_6r_6, 4.83 ± 0.16 cal g^{-1}, is significantly larger than the weighted mean, 4.08 cal g^{-1}, of the enthalpies for c_3 and r_2. The fact that no endotherm is observed when previously scanned protein is rescanned indicates that the denaturation is irreversible, as is also the case with the r_2 and c_3 subunits. Empirical justification for analyzing the data in terms of equilibrium thermodynamics is cited. The observed DSC curves can be expressed within experimental uncertainty as the sum of five sequential two-state steps. The value of $t_{1/2}$, the temperature of half-completion, for each step increases with increasing protein concentration, indicating that some dissociation of the protein takes place during denaturation. Since earlier work [Edge, V., Allewell, N. M., & Sturtevant, J. M. (1985) *Biochemistry 24*, 5899–5906] indicated that neither the regulatory nor the catalytic subunits dissociate on denaturation, the dissociation of c_6r_6 is presumably either to $2c_3 + 3r_2$ or to $2c_3 + r_6$. The effects of ligand concentration on the five steps in the denaturation are complex. The changes in overall denaturational enthalpies produced by the ligands lead to enthalpies of dissociation from the native enzyme as follows: for *N*-(phosphonoacetyl)-L-aspartate, 45 ± 3 kcal mol^{-1}; for ATP, 2.1 ± 0.1 kcal mol^{-1}; and for CTP, −36 ± 4 kcal mol^{-1}.

Aspartate transcarbamoylase (ATCase; aspartate carbamoyltransferase; carbamoyl-phosphate:L-aspartate carbamoyltransferase, EC 2.1.3.2) has been extensively used as a model system for investigating how linkages between ligand binding, conformational transitions, and protein–protein interactions regulate protein function [for recent reviews, see Kantrowitz et al. (1980a,b) and Allewell (1987)]. The enzyme catalyzes the first committed step in pyrimidine biosynthesis, transfer of the carbamoyl moiety of carbamoyl phosphate to the α-amino group of L-aspartate. Both substrates bind cooperatively, and at nonsaturating concentrations, ATP is an

†Supported by National Institutes of Health Grants AM-17335 (N.M.A.) and GM-04725 (J.M.S.) and by National Science Foundation Grant DMB-8421173 (J.M.S.).
*Address correspondence to this author at the Department of Chemistry, Yale University.

0006-2960/88/0427-8081$01.50/0